Magnetic field diagnostics of plasmas based on coherent population trapping: Theory and experiment

Rinat Akhmedzhanov and Ilya Zelensky
Institute of Applied Physics, Russian Academy of Science, 46, Ulyanov Street, Nizhny Novgorod, 603950, Russia

Roman Kolesov and Elena Kuznetsova
Institute of Applied Physics, Russian Academy of Science, 46, Ulyanov Street, Nizhny Novgorod, 603950, Russia
and Department of Physics and Institute for Quantum Studies, Texas A&M University, College Station, Texas 77843-4242, USA
(Received 3 November 2003; published 30 March 2004)

We propose a local, all-optical method of magnetic field diagnostics for plasmas. This method is based on the phenomenon of coherent population trapping in a multilevel medium. The proposed technique allows one to detect both the strength and the orientation of the field. The feasibility of the method was tested in a proof-of-principle experiment in a low-pressure neon discharge.

DOI: 10.1103/PhysRevE.69.036409 PACS number(s): 52.70.Kz, 42.50.Gy, 52.70.Ds

I. INTRODUCTION

A detailed knowledge of the internal magnetic field is of great importance in many plasma configurations. The effect of coherent population trapping (CPT) [1], known for quite a long time in quantum optics, is extremely suitable for local diagnostics of the magnetic field in media containing atoms or ions with magnetic field dependent level splitting. CPT manifests itself in disappearance of resonance fluorescence from a multilevel medium when bichromatic radiation is applied, provided that the frequency difference of the two laser fields exactly matches the frequency of a high-Q (typically, Zeeman or hyperfine) atomic transition. In a closely related effect, called electromagnetically induced transparency (EIT) [2], absorption of a weak probe laser beam is strongly attenuated if another beam of sufficiently high intensity is applied under the condition of two-photon resonance. Even though the two effects are closely related, there is a significant difference between them: EIT is related to field propagation (less absorption along the propagation path), while CPT occurs locally (atoms are not excited by the action of laser fields at the spatial point where the two-photon resonance condition is satisfied). Thus CPT permits spatially localized detection of a magnetic field.

The spectral resolution of the CPT signal is determined by the minimum width of the resonance in a fluorescence signal. It is given basically by the Zeeman sublevel coherence decay rate for the unsaturated CPT limit, when the laser field intensities do not significantly exceed the threshold value necessary for CPT to be established. This threshold intensity is typically lower than the intensity required to saturate an optical transition. The Zeeman coherence decay rate can be orders of magnitude smaller than the optical transition's natural and Doppler widths, which makes the spectral resolution of the CPT signal quite high.

The general idea of the method proposed is illustrated schematically in Fig. 1 and can be explained in the following way. Suppose that two laser beams with close wavelengths propagate in a plasma and intersect at the point of interest, where the magnetic field is to be measured. It is assumed that the plasma contains atoms or ions with an optical transition close to a resonance with the optical field and the ground or/and excited state of this transition is split by the magnetic field into a set of Zeeman sublevels. By adjusting the frequencies of the laser beams, the two-photon resonance condition can be satisfied and a CPT dip in the fluorescence profile will be detected. By measuring the fluorescence spectrum from the intersection volume of the two beams as a function of their frequency shift, the magnetic field magnitude and direction can be deduced from the positions and amplitudes of the CPT resonances, as is shown below. In fact, a similar technique was used recently in two-dimensional (2D) imaging of spatially inhomogeneous magnetic fields, realized experimentally in a Na atomic vapor [3]. It allows one to obtain 2D contours of constant magnetic field in alkali-metal atomic vapors with high field resolution of the order of 1–100 mG.

The aim of this paper is to develop the plasma diagnostics proposed in [4], in particular, to analyze theoretically and experimentally the possibility of measuring both magnetic field strength and direction by using CPT. The applicability to typical experimental plasmas is also discussed.

II. THEORETICAL BACKGROUND

The simplest atomic system suitable for the technique is a four-level system, depicted in Fig. 2, where the upper level is a singlet and the lower level is a triplet state. An external magnetic field splits it into three Zeeman sublevels with level separation equal to the Larmor frequency $\omega_L = g\mu_B B/\hbar$. Here g is the Landé factor of the lower level, μ_B is the Bohr magneton, and B is the magnetic field strength.

Consider two electromagnetic waves E_1 and E_2 with frequencies ω_1 and ω_2, respectively, both propagating in the z direction. The waves are linearly polarized such that either $\mathbf{E}_1, \mathbf{E}_2 \| \hat{\mathbf{e}}_x$ or $\mathbf{E}_1, \mathbf{E}_2 \| \hat{\mathbf{e}}_y$ with $\hat{\mathbf{e}}_i$ being the unit vector of the i polarization. The arbitrarily oriented magnetic field is described by the angles α and β (see Fig. 3). We choose the quantization axis along $\mathbf{k} \| \hat{\mathbf{e}}_z$.

For a given magnetic field, depending on the selection rules for the angular momentum, which are determined by the laser field polarizations and magnetic field orientation,

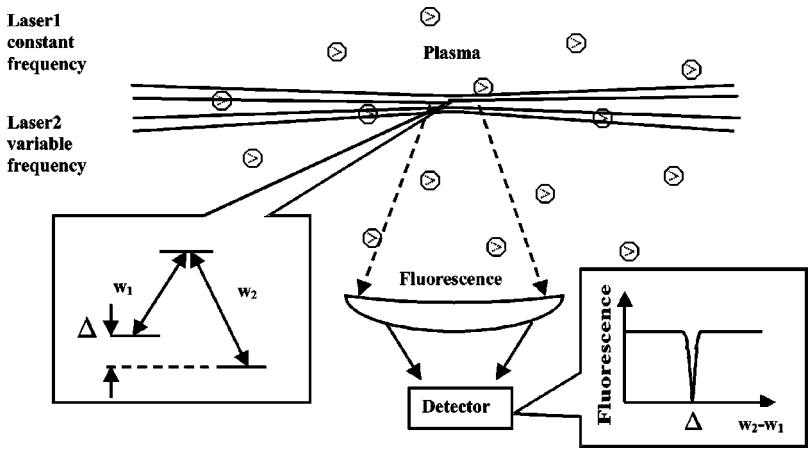

FIG. 1. Schematic of the diagnostic method.

CPT resonances will be observed in a fluorescence spectrum whenever the two-photon resonance condition is satisfied:

$$\omega_1-\omega_2=\pm\omega_L,\pm 2\omega_L.$$

In the case that **B** is along **k**, each linearly polarized e.m. field can be decomposed into a combination of σ^+ and σ^- components, for which only transitions with $\Delta m=\pm 1$ are respectively allowed. Therefore, if the two-photon detuning is varied, only the CPT resonance at the double Larmor frequency, when $\omega_1-\omega_2=\pm 2\omega_L$, will be observed [Fig. 2(a)]. The situation is changed if the magnetic field is tilted with respect to **k** such that it now has a projection on the e.m. wave polarization direction. In this case selection rules also allow for the transition with $\Delta m=0$ due to the fact that the e.m. fields now have an admixture of a π component. As a result an additional resonance appears at the single Larmor frequency $\omega_1-\omega_2=\pm\omega_L$ [Fig. 2(b)]. A theoretical analysis of the interaction of two laser fields with the four-level system depicted in Fig. 2(a) shows that the magnetic field orientation can be determined from the ratio of the fluorescence intensities of the CPT resonances at single and double Larmor frequencies. The main assumptions used in the analysis are (1) the laser field intensities do not significantly exceed the CPT saturation limit; (2) the Doppler width of the optical transition exceeds the Zeeman splitting; (3) the homogeneous linewidth of the transition is smaller than the Zeeman splitting; (4) an average over the distribution of optical transition frequencies due to the Doppler effect is carried out.

The fluorescence intensity is proportional to a steady-state upper level population ρ_{44}. In the Λ system of Fig. 2(a) formed by the σ^- component of the first field and the σ^+ component of the second field, ρ_{44} is proportional to the product of the intensities of the laser fields resonantly applied to the arms of the system, each intensity being multiplied by the strength of the corresponding transition, given by the square of the dipole moment:

$$\rho_{44}\sim I_1|\mu_{41}^1|^2 I_2|\mu_{43}^2|^2\sim|\Omega_1^{41}|^2|\Omega_2^{43}|^2,$$

where I_1 and I_2 are the laser field intensities, μ_{41}^1 and μ_{43}^2 are the dipole moments of the $4\rightarrow 1$ and $4\rightarrow 3$ transitions, which take into account the field polarizations, and the Rabi frequencies of the laser fields are

$$\Omega_j^{4i}=\frac{\mu_{4i}^j E_j}{2\hbar}=\frac{\mu E_j}{2\hbar}f_{4i}(\alpha,\beta)=\Omega_j f_{4i}(\alpha,\beta),$$

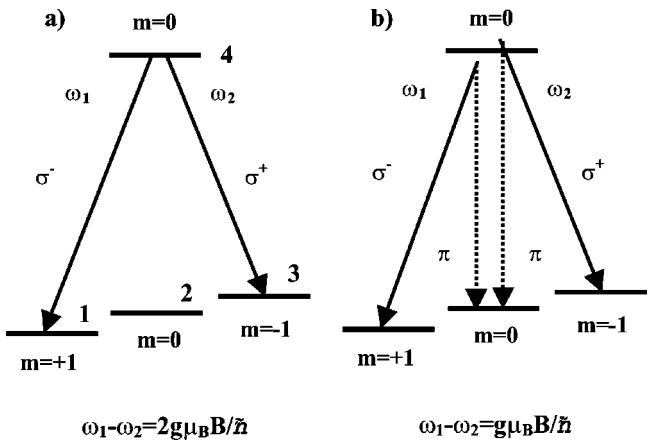

FIG. 2. Laser-coupling schemes, showing CPT resonance configurations in the atomic system studied in the experiment.

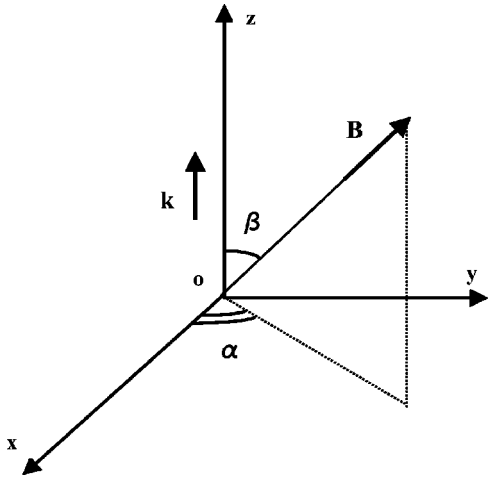

FIG. 3. Magnetic field orientation.

where the indices $i=1,2,3$ and $j=1,2$ denote the Zeeman sublevels of the lower level and laser fields, respectively; μ contains an integral over the radial parts of the lower and upper state wave functions; $\Omega_j=\mu E_j/2\hbar$ are the angular independent Rabi frequencies of the laser fields; and $f_{4i}(\alpha,\beta)$ gives the angular dependence of the dipole moment. For identical polarizations f_i is the same for E_1 and E_2.

In the case of resonance at the single Larmor frequency, shown in Fig. 2(b), two Λ schemes are formed by the $\sigma^{-(+)}$ and π components of the fields. These Λ schemes are resonant with different groups of atoms symmetrically Doppler-shifted with respect to the central frequency of the optical transition. The two groups give contributions to ρ_{44} proportional to $|\Omega_1^{41}|^2|\Omega_2^{42}|^2$ and $|\Omega_1^{42}|^2|\Omega_2^{43}|^2$, respectively. In the unsaturated CPT limit, when $|\Omega_1|^2+|\Omega_2|^2\sim\Gamma W_D$ (Γ is the Zeeman coherence decay rate and W_D is the optical transition Doppler linewidth [5]), the proportionality coefficients containing information about the resonance profiles turn out to be identical for the three Λ systems considered above.

The ratio of the fluorescence intensities is then given by the following expression:

$$r=\frac{I^{w_1-w_2=w_L}}{I^{w_1-w_2=2w_L}}=\frac{|\Omega_1^{41}|^2|\Omega_2^{42}|^2+|\Omega_1^{42}|^2|\Omega_2^{43}|^2}{|\Omega_1^{41}|^2|\Omega_2^{43}|^2}. \qquad (1)$$

For the case $\mathbf{E}_1,\mathbf{E}_2\|\hat{\mathbf{e}}_x$,

$$f_{41}=-f_{43}^*=i\sin\alpha+\cos\alpha\cos\beta,$$

$$f_{42}=-\sqrt{2}\sin\beta\cos\alpha.$$

The ratio of intensities (1) has the form

$$r_x=\frac{4\sin^2\beta}{\tan^2\alpha+\cos^2\beta}.$$

For the case $\mathbf{E}_1,\mathbf{E}_2\|\hat{\mathbf{e}}_y$,

$$f_{41}=-f_{43}^*=-i\cos\alpha+\sin\alpha\cos\beta,$$

$$f_{42}=-\sqrt{2}\sin\beta\sin\alpha.$$

The time the ratio (1) is given by

$$r_y=\frac{4\sin^2\beta}{\cot^2\alpha+\cos^2\beta}.$$

From r_x and r_y one can determine $\cos^2\beta$ and $\tan^2\alpha$. This gives one four possible directions of the magnetic field. In order to choose the right one, some additional knowledge about the magnetic field geometry is required. The advantage of this method is that $r_{x(y)}$ is independent of the intensities of the fields and is determined only by the geometry of the experiment.

III. EXPERIMENTAL RESULTS

To demonstrate the feasibility of the described technique we performed a proof-of-principle experiment in a plasma of a low-pressure glow neon discharge. The neon atomic energy levels are shown in Fig. 4. The electric-dipole-allowed transition $2p^53s\ ^3P_1(J=1)\rightarrow 2p^53p\ ^3P_0(J=0)$ of wavelength 607.4 nm was chosen for a number of reasons: (1) it is within the wavelength range of a typical dye laser; (2) the simple four-level structure allows analytical expressions for CPT parameters be derived, as was shown in the previous section; (3) the lower level has $J=1$ (with the Landé factor $g=1.464$) and decays radiatively to the ground state with a decay rate $\sim$9 MHz, comparable to that of the upper level. This makes the Zeeman coherence lifetime of the same order as the time required to establish CPT. Therefore, it is important to verify that the technique will work even in such unfavorable conditions.

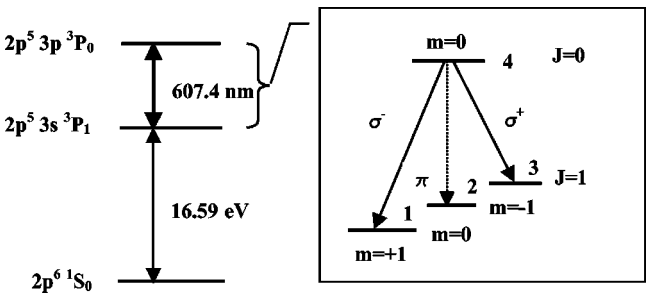

FIG. 4. Energy level diagram of a Ne atom. In the inset selection rules for different polarizations of laser fields are depicted.

The experimental setup used in the present experiment is illustrated schematically in Fig. 5. A single-mode dye laser output at 607.4 nm, tuned to the $2p^53s^3P_1\rightarrow 2p^53p^3P_0$ transition of a Ne atom, was split into two beams. The frequency of one beam was shifted by an acousto-optic modulator (AOM) by $\Delta\omega=110$ MHz. After being recombined the beams were propagated along the axis of a discharge tube. A tube with a neon glow discharge (Ne pressure 1.5 Torr, discharge current 40 mA) was placed into an external magnetic field. Its longitudinal component $\mathbf{B}_l$ was produced by a solenoid and the transverse component $\mathbf{B}_{\rm tr}$ by Helmholtz coils. The Zeeman splitting was varied for given laser field frequencies by sweeping the longitudinal component of the magnetic field. The sweeping frequency was tuned in the range 20–40 Hz to minimize low-frequency noise. It is worth noting that the discharge parameters were slightly modulated by the alternating magnetic field. Fluorescence emitted from the discharge in the direction perpendicular to the laser beam propagation direction was separated by a monochromator and detected by a photomultiplier. The laser

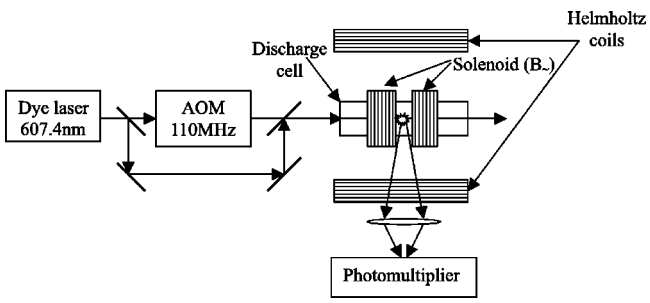

FIG. 5. Experimental setup.

fields had identical linear polarizations, which could be rotated to be either parallel or perpendicular to $\mathbf{B}_{\mathrm{tr}}$. The powers of the laser beams were equal (approximately 2.5 mW in each beam) with a beam spot of ~1 mm in diameter; the resulting intensities correspond to the unsaturated CPT regime, so power broadening of resonances is not expected in the experiment.

In the course of the experiment we set $\mathbf{B}_{\mathrm{tr}} \| \mathbf{Ox}$, which corresponds to $\alpha = 0$ in the notation of Fig. 3. According to Eq. (1) this gives

$$r_x = 4 \tan^2 \beta = 4 \frac{B_{\mathrm{tr}}^2}{B_l^2}, \quad r_y = 0; \tag{2}$$

the last result means that no CPT resonance at the single Larmor frequency will be observed if $\mathbf{E}_1, \mathbf{E}_2 \| \hat{\mathbf{e}}_y$, since in this case the magnetic field is perpendicular to the laser beam polarization.

A series of CPT spectra in the presence of a static transverse magnetic field is shown in Fig. 6. The magnitude of the transverse field is given in terms of the current I through the Helmholtz coils. In the case of small B_{tr} ($I \leqslant 200$ mA) CPT dips are observed only at frequency shifts $\omega_1 - \omega_2 = 0, \pm 2\omega_L$. The resonance at zero shift, which is due to formation of CPT in a degenerate Λ system, is of no interest for us since it carries no information about the magnetic field. As the current is increased, the resonance at the single Larmor frequency $\omega_1 - \omega_2 = \pm \omega_L$ appears.

The position of the CPT dip at the double Larmor frequency for $I = 0$ ($B_{\mathrm{tr}} = 0$) gives the total magnetic field magnitude for a fixed laser beam frequency difference:

$$B_{\mathrm{tot}} = B_l = \frac{\Delta \omega \hbar}{2 g \mu_B}. \tag{3}$$

In our case for $\Delta\omega = 110$ MHz the resonance was detected for $B_{\mathrm{tot}} = 26.2$ G. As can be seen from Fig. 6, it shifts to smaller values of B_l as B_{tr} increases, as expected. Eventually, for currents greater 550 mA, the resonance strongly overlaps with the resonance at $B_l = 0$ and is no longer detectable.

As can be seen from Fig. 6, the width of the resonance at $\omega_1 - \omega_2 = 2\omega_L$ in the absence of the transverse field ($I = 0$) is ~10 G, which corresponds to a spectral full width at half maximum ~42 MHz. This means that the Zeeman coherence decay rate in our experiment, given by one-half of this value, is ~21 MHz. It is the sum of the radiative decay rate of 9 MHz and the collisional decay rate, which turns out to be 12 MHz, due to collisions with ground-state neon atoms. Although the Zeeman coherence decay rate is two times larger than the radiative decay rate of the upper level, the resonances are still detectable.

In order to test the validity of Eq. (2), we calculated B_{tr} from the ratio r_x of intensities of CPT resonances observed in the experiment. It should be stressed here that, if the frequency shift $\Delta\omega$ is varied for a fixed magnetic field magnitude and orientation, then the use of Eq. (2) is straightforward: B_{tot} is determined from the position of the CPT dip at either the double or single Larmor frequency, and B_{tr} and B_l are calculated from r_x according to the following expressions:

$$B_l = 2 B_{\mathrm{tot}} \sqrt{1/(4 + r_x)},$$

$$B_{\mathrm{tr}} = B_{\mathrm{tot}} \sqrt{r_x/(4 + r_x)}.$$

In the experiment B_l was swept for fixed $\Delta\omega$; therefore Eq. (2) has to be modified to give the correct values of B_{tr}. As is illustrated in Fig. 7, CPT resonances at single and double Larmor frequencies occur for different values of B_{tot} and β. To take this into account we turn to the original expression (1) for r_x, which gives

$$r_x = \frac{4 \cos^2 \beta_2 \sin^2 \beta_2}{\cos^4 \beta_1} = \frac{4[B_{\mathrm{tr}}/(\Delta\omega\hbar/g\mu_B)]^2 \{1 - [B_{\mathrm{tr}}/(\Delta\omega\hbar/g\mu_B)]^2\}}{\{1 - 4[B_{\mathrm{tr}}/(\Delta\omega\hbar/g\mu_B)]^2\}}.$$

From this expression B_{tr} is derived:

$$B_{\mathrm{tr}} = \frac{\Delta\omega\hbar}{g\mu_B} \sqrt{(2r_x + 1 - \sqrt{3r_x + 1})/2(4r_x + 1)}. \tag{4}$$

The spectra in Fig. 6 were fitted with several Lorentzians, one Lorentzian for each CPT peak, two Lorentzians for the resonance at $B_l = 0$, and one for a smooth background. The amplitudes of the Lorentzians were used as the intensities of the CPT resonances. The resulting dependence of B_{tr}, calculated according to Eq. (4), on the current I through the Helmholtz coils is presented in Fig. 8. The dependence is linear, as expected; the slope 30.2 G/A of the linear fit to this dependence agrees well with the magnetic constant 31.7 G/A of the Helmholtz coils, obtained from an independent measurement by a magnetometer.

IV. DISCUSSION

The magnetic field measurement accuracy in the proposed technique is determined by the spectral resolution of the CPT signal. It is usually very high, depending neither on the Doppler and natural linewidths of the optical transition, nor on the laser linewidth provided the two beams are from the same laser source. In the unsaturated CPT case the spectral resolution is given by the Zeeman coherence decay rate Γ. For a metastable lower level this rate can be of the order of 100 kHz and the corresponding field resolution is hundreds of milligaus; for a radiative lower level (as is the case for the transition studied) the decoherence rate is 1–10 MHz, and the corresponding resolution is lower—several gauss. It is worth noting that excited states are strongly influenced by collisions. Thus the Zeeman coherence decay rate in the limit of unsaturated CPT provides information about collisional rates, if the decoherence collisional mechanisms are known. This method does not have any major limitations on the strength of the magnetic field; the only difficulty in the case of large fields, leading to large Zeeman splittings, is in phase locking the laser fields if they come from different sources,

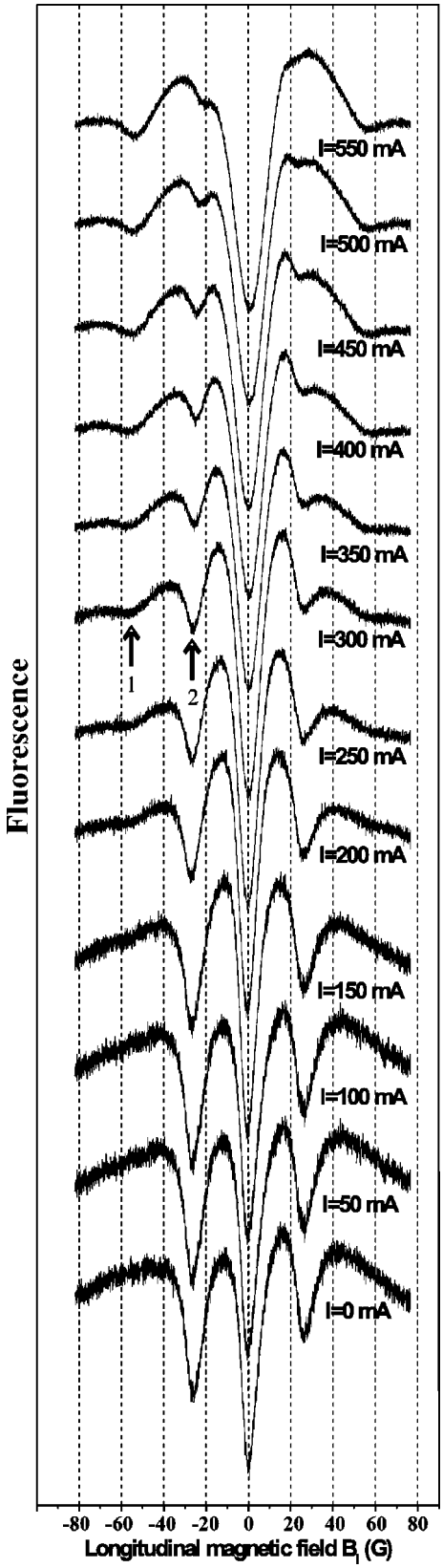

FIG. 6. Experimental fluorescence intensity dependences on the longitudinal component B_l for a number of values of the transverse component B_{tr}, expressed in terms of the current I through the Helmholtz coils; resonance at (1) $\omega_1-\omega_2=\omega_L$; (2) $\omega_1-\omega_2=2\omega_L$.

but currently available optical methods solve this problem [6]. This technique, though, is particularly advantageous for measuring small magnetic fields (up to 1 kG), which are difficult to detect using conventional spectroscopic plasma diagnostics, since they produce a tiny Faraday rotation and Zeeman splittings much smaller than the Doppler width of any optical line.

The technique allows one to study nonstationary processes. The temporal resolution is given by the CPT preparation time. This time, in turn, is proportional to the radiative lifetime of the upper optical level. For a typical electric-dipole-allowed transition with oscillator strength $f\sim 1$ the radiative lifetime is $\tau\sim 10-100$ ns. The temporal resolution $\sim 10\tau\sim 0.1-1$ μs is obtained from the requirement that the CPT has enough time to form.

It is essential also that the time required to establish CPT be smaller than the Zeeman coherence lifetime, otherwise the effect is not observed. This imposes a limit on the rates of decoherence processes in the plasma of interest.

There is a requirement that the signal-to-noise ratio suffices to reliably detect CPT resonances. This gives the minimum density of test particles and determines the spatial resolution. Let us analyze it for an experimental situation where the main source of noise is the background plasma emission on the resonant wavelength. During the detection time $\Delta\tau$ the number of resonantly emitted photons is N_r, while the background plasma produces N_{pl} spontaneous photons. A useful fluorescence signal is reliably detected if its intensity sufficiently exceeds the root-mean-square value of the noise $\sqrt{N_{\mathrm{pl}}}$:

$$N_r \geqslant 3\sqrt{N_{\mathrm{pl}}}. \tag{5}$$

The number of resonantly emitted photons is proportional to the volume l^3 with l being the required spatial resolution, while N_{pl} originates from the whole plasma volume l^2L along the collection optics field of view, where L is the characteristic scale of the plasma. The condition (5) can be rewritten in the following form [4]:

$$\sqrt{Al^4\Omega_{\mathrm{solid}}\eta t\Delta\tau/4\pi L}\,\frac{\Delta N_{\mathrm{up}}}{\sqrt{N_{\mathrm{up}}}} \geqslant 3, \tag{6}$$

where A is the radiative decay constant of the upper state, $\Omega_{\mathrm{solid}}/4\pi$ is the solid angle observed by the collection optics, η is the quantum efficiency of the photodetector, t is the transmission coefficient of the collection optics, N_{up} is the density of spectroscopic particles excited by the discharge to the upper level, and ΔN_{up} is the increase of the upper level population density due to the action of the lasers.

Let us analyze the last two limitations of the method separately for cold and hot plasmas. For cold, partially ionized plasmas, typically found in different types of discharges, this technique is expected to be particularly useful due to the low values of the magnetic field ($\leqslant$0.2–0.3 T), where application of other diagnostics may be difficult. These discharges are characterized by ion temperatures in the range of 0.025–5 eV, electron temperatures from 1 to 20 eV, and ion or electron densities of 10^9-10^{12} cm^{-3}. In such plasmas neutral at-

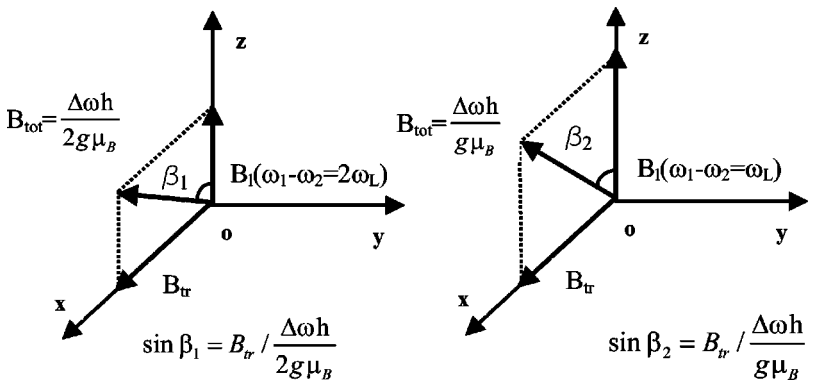

FIG. 7. Difference in magnetic field magnitude and orientation between two types of CPT resonance observed in the experiment.

oms might be used as test particles. The Zeeman coherence decays mainly due to neutral-neutral collisions, with a rate of $\nu_{\text{neut}}=\sigma N_{\text{neut}} v^T_{\text{neut}}$, where $\sigma\sim 8\times 10^{-15}$ cm^2 is the coherence-destroying collision cross section for a radiative level [7] (for a metastable level it is typically lower), N_{neut} is the density of neutral atoms, and the thermal velocity $v^T_{\text{neut}}=\sqrt{3kT/m}\sim 3\times 10^4-10^6$ cm/s. The collisional rate will be less than $\tau^{-1}=10$ MHz for $N_{\text{neut}}<10^{16}-4\times 10^{17}$ cm^{-3}, which corresponds to pressures of several Torrs.

Let us turn now to the signal-to-noise ratio calculation. In Eq. (6) we assume that the upper level population density increase by the laser action is of the order of the initial density difference between the lower and upper states, $\Delta N_{\text{up}}\simeq N_{\text{low}}-N_{\text{up}}$. The population densities of the upper and lower states are calculated from the requirement of a balance between the excitation processes due to inelastic collisions with electrons, which have a significantly larger temperature in comparison with atoms, and radiative processes. We use the model of a test plasma atom, which includes the ground and two excited states, as depicted in Fig. 9, neglecting excitation into higher-lying excited states.

The population densities are easily calculated:

$$N_{\text{up}}=\nu^e_{lu}N_{\text{low}}/A,$$

$$N_{\text{low}}=\nu^e_{gl}N_0/A_g,$$

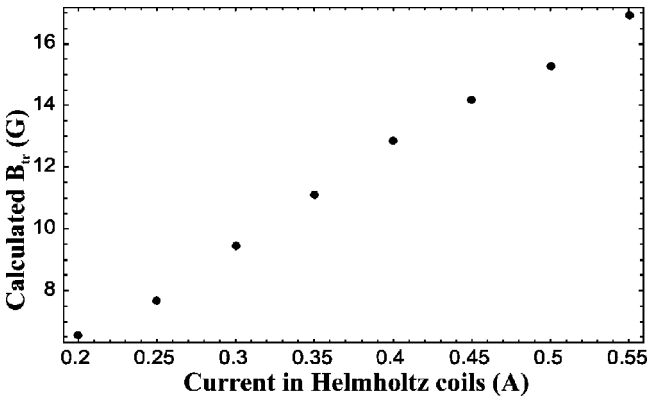

FIG. 8. B_{tr} calculated from experimental CPT spectra according to Eq. (4).

where N_0 is the population density of the ground state. The excitation rates due to inelastic collisions with electrons are [8]

$$\nu^e_{gl}=3.2\times 10^{-7} f_{gl}\left(\frac{\mathcal{R}y}{E_{\text{low}}}\right)^{3/2}\times e^{-E_{\text{low}}/kT_e}\sqrt{E_{\text{low}}/kT_e}\,p(E_{\text{low}}/kT_e)N_e,$$

$$\nu^e_{lu}=3.2\times 10^{-7} f_{lu}\left(\frac{\mathcal{R}y}{\Delta E}\right)^{3/2}\times e^{-\Delta E/kT_e}\sqrt{\Delta E/kT_e}\,p(\Delta E/kT_e)N_e. \quad (7)$$

Here $f_{gl,lu}$ is the oscillator strength of the $|g\rangle\rightarrow|\text{lower}\rangle$, $|\text{lower}\rangle\rightarrow|\text{upper}\rangle$ transition, E_{low} is the energy of the lower state, ΔE is the energy difference between the lower and the upper states, kT_e is the electron temperature in eV, $\mathcal{R}y=13.6$ eV, and N_e is the electron density in cm^{-3}. We take the values $kT_e=10$ eV and $N_e=10^{10}$ cm^{-3}, typical for a cold plasma, the typical energies $E_{\text{low}}\sim 15$ eV, and $\Delta E\sim 2-5$ eV, and the radiative decay constants $A, A_g\sim 10^7-10^8$ s^{-1}, typical for an electric-dipole-allowed transition ($f_{gl,lu}\sim 1$). The p function is equal to 0.1 for the $|g\rangle\rightarrow|\text{lower}\rangle$, and 0.3 for $|\text{lower}\rangle\rightarrow|\text{upper}\rangle$ transitions. This gives excitation rates $\nu^e_{gl}\approx 100$ s^{-1} and $\nu^e_{lu}\approx(2-6)\times 10^3$ s^{-1}. We then have

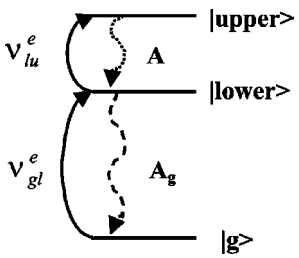

FIG. 9. Illustration of the calculation of population densities of upper and lower states. Here A and A_g are radiative decay constants of the lower and upper levels, and ν^e_{gl} and ν^e_{lu} are the excitation rates due to inelastic collisions with electrons.

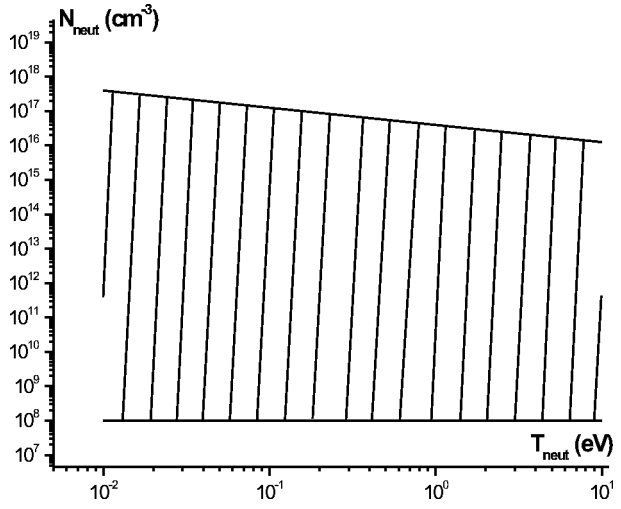

FIG. 10. The hatched area shows the approximate range of cold plasma parameters where the method works.

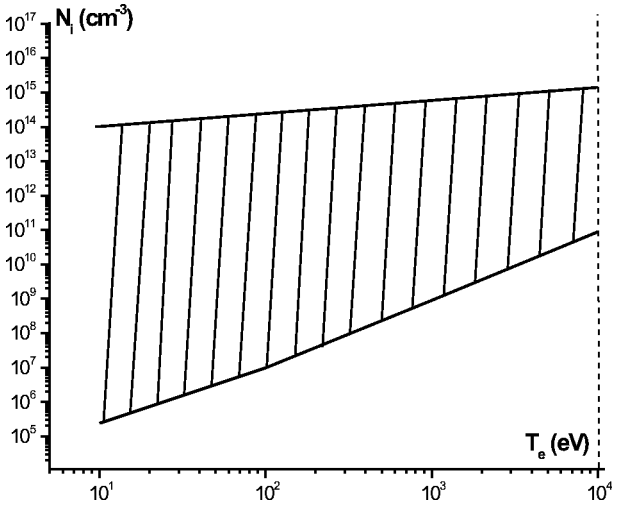

FIG. 11. Hatched is the range of hot plasma parameters where the diagnostic is applicable. $T_i = T_e$ was assumed in calculations.

$$\frac{\Delta N_{\rm up}}{\sqrt{N_{\rm up}}} \sim \frac{N_{\rm low} - N_{\rm up}}{\sqrt{N_{\rm up}}} = \sqrt{N_0}\sqrt{\nu^e_{gl}/A_g / \nu^e_{lu}/A}(1 - \nu^e_{lu}/A) \sim \sqrt{N_0}\sqrt{\nu^e_{gl}/\nu^e_{lu}} \approx (0.1-0.2)\sqrt{N_0}.$$

This allows us to estimate the minimum density of test particles required by the need for an adequate signal-to-noise ratio. Putting into Eq. (6) the typical parameters of a collection system ($\Omega_{\rm solid}/4\pi \sim 10^{-2}$, $\eta \sim 10^{-2}$, $t = 0.5$), the characteristic plasma scale $L = 1$ m, and spatial and temporal resolution $l \sim 1$ cm and $\Delta\tau \sim 1\ \mu$s, we get $N_0 \geqslant 10^7 - 10^8$ cm^{-3}. The range of parameters of a cold plasma at which the technique is applicable, calculated according to the model we used above, is depicted in Fig. 10.

In hot, fully ionized plasmas, ions might be used as test particles. If the temperature of a plasma is very high, the main source of Zeeman decoherence is the particle flight out of the laser beam, and it sets a limit on the thermal velocity of the atoms or ions; namely, the time of flight of a spectroscopic particle through the laser beam has to exceed the CPT preparation time, $\tau < l/v^T$, where l is the laser beam diameter and v^T is the thermal velocity. For $l = 1$ cm and $\tau = 10$ ns, the maximum velocity is $v^T < 10^6$ m/s, or, equivalently, the maximum temperature $T < 10$ keV (here and in the rest of the text the mass $m \sim 10 m_p$ is used in estimates). The main coherence dephasing mechanism at smaller temperatures is ion-ion and ion-electron collisions. For an estimate, we use integrated ion-ion and ion-electron elastic collision rates [9]:

$$\nu_{ii} = \frac{16\pi e^4 Z^4 N_i L_i}{(3kT_i)^{3/2} m_i^{1/2}}, \tag{8}$$

$$\nu_{ei} = \frac{4\pi e^4 Z^2 N_e L_e}{(3kT_e)^{3/2} m_e^{1/2}}. \tag{9}$$

Here N_i and N_e are the ion and electron densities, m_i and m_e are their masses, Z is the ion charge number, $L_i = 23 + 3/2 \ln T_{i,e} - 1/2 \ln N_i$, $L_e = 24 + \ln T_e - 1/2 \ln N_e$ for $T_e > 10$ eV [Coulomb logarithms; $T_{i,e} = \min(T_i, T_e)$, T_i, T_e are in eV, N_i, N_e are in cm^{-3}]. The rate of inelastic collisions with electrons can be estimated using Eq. (7). For an estimate we take $L_i = L_e = 10$, $T_i = T_e = 10 - 10^4$ eV, and $Z = 1$. The condition ν_{ii}, ν_{ei}, $\nu^e_{lu} < 10$ MHz is satisfied for ion and electron densities $N_i, N_e < 10^{14} - 10^{15}$ cm^{-3}. The higher the electron or ion temperature, the higher are the ion and electron densities allowed, as is clear from Eqs. (7)–(9).

Let us now estimate from Eq. (6) the minimum ion density required to discriminate a signal against noise. Supposing a thermalized plasma, we have $\Delta N_{\rm up} \simeq N_{\rm low} - N_{\rm up} = N_0 \exp(-E_{\rm low}/kT)[1 - \exp(-\Delta E/kT)]$. The condition (6) assumes the form

$$\sqrt{A l^4 \Omega_{\rm solid} \eta t \Delta\tau N_0 / \pi L} \times \exp(-E_{\rm low}/2kT) \sinh(\Delta E/2kT) \geqslant 3.$$

Let us estimate the detection limit for the case of high temperature, which is obviously the worst from the signal-to-noise point of view due to the almost equal population of levels by the discharge. For the same parameters of the collection system, plasma scale, spatial and temperature resolution, for a dipole-allowed optical transition with $\Delta E = 2 - 5$ eV, and taking the electron and ion temperature $T = 10 - 10^4$ eV, the detection limit is $N_0 \geqslant 10^5 - 10^{10}$ cm^{-3}. This reasoning is summarized in Fig. 11.

V. CONCLUSION

A local magnetic field diagnostics based on the coherent population trapping effect has been developed. The diagnostics is an extension of the laser induced fluorescence technique, providing sub-Doppler and subnatural spectral resolution by the use of a two-photon Raman transition. The high spectral resolution of the CPT signal, determined by the Zeeman sublevel coherence decay rate, leads to a high magnetic

field measurement accuracy, nicely combined with good temporal and spatial resolution. The technique is able to measure both the strength and the orientation of the field.

A demonstration experiment was carried out in a plasma produced in a low-pressure neon glow discharge. It was shown that from the position of a CPT resonance in the fluorescence spectrum the strength of the local magnetic field can be obtained. By utilizing the dependence of the dipole moments of optical transitions from different Zeeman sublevels of a lower level to a common upper level on magnetic field orientation and laser field polarizations, it was demonstrated that the direction of the field can be determined from the ratio of the fluorescence intensities of the two types of CPT resonance. We made theoretical estimates of the range of temperatures and densities for cold and hot plasmas where the technique can be applied. The estimates show that the technique is applicable to a variety of plasma configurations. It might be particularly useful in magnetic confinement devices with low magnetic fields, where application of other diagnostics may be difficult.

ACKNOWLEDGMENTS

We are grateful to Olga Kocharovskaya, Alexander Kostrov, Aleksandr Litvak, Vyacheslav Mironov, Yuri Rostovtsev, and Farit Vagizov for useful discussions. We also acknowledge financial support by the Russian Foundation for Basic Research (Grant Nos. 01-02-17779, 03-02-17176, and 03-02-17234), the Texas Advanced Technology and Research Program, the Office of Naval Research, and the Defense Advanced Research Project Agency.

[1] E. Arimondo, Prog. Opt. **35**, 257 (1996).
[2] S. E. Harris, Phys. Today **50**(7), 36 (1997).
[3] H. Asahi, K. Motomura, K.-I. Harada, and M. Mitsunaga, Opt. Lett. **28**, 1153 (2003).
[4] P. M. Anisimov, R. A. Akhmedzhanov, I. V. Zelensky, R. L. Kolesov, and E. A. Kuznetsova, Zh. Eksp. Teor. Fiz. **96**, 801 (2003) [JETP **123**, 912 (2003)].
[5] E. Kuznetsova, O. Kocharovskaya, P. R. Hemmer, and M. O. Scully, Phys. Rev. A **66**, 063802 (2002).
[6] T. Udem *et al.*, Phys. Rev. Lett. **79**, 2646 (1997); J. Reichert *et al.*, *ibid.* **84**, 3232 (2000).
[7] R. J. McLean, R. J. Ballagh, and D. M. Warrington, J. Phys. B **18**, 2371 (1985).
[8] I. I. Sobelman, L. A. Vainshtein, and E. A. Yukov, *Excitation of Atoms and Broadening of Spectral Lines* (Springer-Verlag, Berlin, 1981).
[9] V. E. Golant, A. P. Zhilinsky, and S. A. Sakharov, *Fundamentals of Plasma Physics* (Wiley, New York, 1980).